

DRAGON: LLM-Driven Decomposition and Reconstruction Agents for Large-Scale Combinatorial Optimization

Shengkai Chen

Institute for Infocomm Research
A*STAR, Singapore
Chen_Shengkai@a-star.edu.sg

Yaoxin Wu

Eindhoven University of Technology
Eindhoven, Netherlands
y.wu2@tue.nl

Xiaoli Li

Singapore University of Technology
and Design, Singapore
xiaoli_li@sutd.edu.sg

Zhiguang Cao

Singapore Management University
Singapore
zgcao@smu.edu.sg

Senthilnath Jayavelu

National University of Singapore,
Institute for Infocomm Research
A*STAR, Singapore
J_Senthilnath@a-star.edu.sg

Jianan Zhou

Nanyang Technological University
Singapore
jianan004@e.ntu.edu.sg

Zhuoyi Lin*

Institute for Infocomm Research
A*STAR, Singapore
Lin_Zhuoyi@a-star.edu.sg

ABSTRACT

Large Language Models (LLMs) have recently shown promise in addressing combinatorial optimization problems (COPs) through prompt-based strategies. However, their scalability and generalization remain limited, and their effectiveness diminishes as problem size increases, particularly in routing problems involving more than 30 nodes. We propose DRAGON, which stands for **D**ecomposition and **R**econstruction **A**gents **G**uided **O**ptimizatioN, a novel framework that combines the strengths of metaheuristic design and LLM reasoning. Starting from an initial global solution, DRAGON autonomously identifies regions with high optimization potential and strategically decompose large-scale COPs into manageable subproblems. Each subproblem is then reformulated as a concise, localized optimization task and solved through targeted LLM prompting guided by accumulated experiences. Finally, the locally optimized solutions are systematically reintegrated into the original global context to yield a significantly improved overall outcome. By continuously interacting with the optimization environment and leveraging an adaptive experience memory, the agents iteratively learn from feedback, effectively coupling symbolic reasoning with heuristic search. Empirical results show that, unlike existing LLM-based solvers limited to small-scale instances, DRAGON consistently produces feasible solutions on TSPLIB, CVRPLIB, and Weibull-5k bin packing benchmarks, and achieves near-optimal results (0.16% gap) on knapsack problems with over 3M variables. This work shows the potential of feedback-driven language agents as a new paradigm for generalizable and interpretable large-scale optimization.

Zhuoyi Lin is the corresponding author.

Shili Xiang

Institute for Infocomm Research
A*STAR, Singapore
Xiang_Shili@a-star.edu.sg

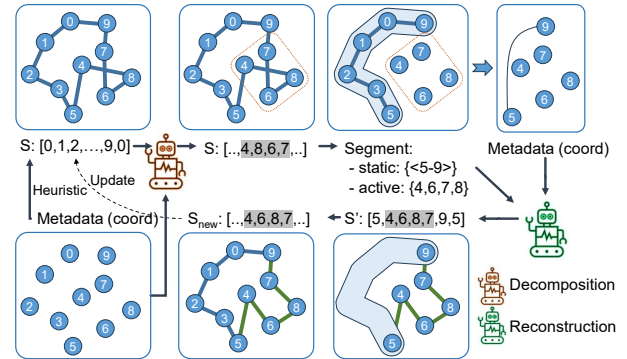


Figure 1: Illustration of DRAGON on a TSP instance, where metadata represent the coordinates of locations to visit, serving as the main environment for the agents. The decomposer identifies a suboptimal active segment $\{4,6,7,8\}$ (grayed) from a global solution. The segment is locally refined and reintegrated by the reconstructor to improve the global tour.

KEYWORDS

Combinatorial Optimization, Large-scale, Metaheuristics

ACM Reference Format:

Shengkai Chen, Zhiguang Cao, Jianan Zhou, Yaoxin Wu, Senthilnath Jayavelu, Zhuoyi Lin*, Xiaoli Li, and Shili Xiang. 2026. DRAGON: LLM-Driven Decomposition and Reconstruction Agents for Large-Scale Combinatorial Optimization. In *Proc. of the 25th International Conference on Autonomous Agents and Multiagent Systems (AAMAS 2026)*, Paphos, Cyprus, May 25 – 29, 2026, IFAAMAS, 21 pages.

1 INTRODUCTION

Combinatorial optimization problems (COPs), such as the Traveling Salesman Problem (TSP), Vehicle Routing Problem (VRP), and Knapsack Problem (KP), are notoriously challenging due to their NP-hard nature [4]. These COPs are typically addressed using exact

algorithms or heuristic methods, which often require substantial manual design and parameter tuning [9, 14, 22, 25, 32], thereby limiting their scalability and adaptability to varying problem instances and domains.

Large Language Models (LLMs) have led to a series of breakthroughs for various challenging problems in natural language processing and artificial intelligence, including language understanding, text generation, code synthesis, and reasoning tasks [1, 8, 10]. Recent evidence reveals that LLMs have emerged as powerful tools capable of addressing a variety of COPs, leveraging their reasoning capabilities for direct solution generation [37, 41] or heuristic design [23, 33, 42, 45]. Their inherent strengths in abstraction, generalization, and semantic understanding allow them to generate promising solutions even without explicit algorithmic instructions. However, despite these advances, the current capabilities of LLMs for directly generating solutions remain largely confined to relatively small-scale instances, such as the TSP with fewer than 30 nodes [17, 24, 41]. As problem size and complexity grow, LLM-based solutions often deteriorate due to inherent limitations, including restricted context length, reduced logical coherence, and difficulty in representing combinatorial structures [17, 43]. These limitations significantly impede the practical deployment of LLM-driven methods in realistic large-scale applications, such as logistics, transportation, and supply chain management, where problems commonly involve hundreds to thousands of nodes [7].

In this study, we aim to answer two research questions: (1) *Can an LLM agent, without solving the full COP, identify and isolate regions of the solution that are likely suboptimal or have improvement potential?* (2) *Can an LLM agent effectively solve small-scale COPs locally while following additional, customized non-trivial constraints?* These questions highlight the core challenges of our framework: utilizing LLMs to guide decomposition by detecting potential improvement areas, and ensuring reconstructed solutions remain feasible.

Prompt-based LLM methods often fail on large-scale instances due to the absence of domain knowledge and the context length limitation, while code-generation approaches require extensive task-specific training to develop robust heuristics, leading to substantial computational costs and poor cross-domain transferability. Meanwhile, classical metaheuristics such as divide-and-conquer and large neighborhood search (LNS) [29] exhibit strong scalability in large-scale COPs by iteratively decomposing and refining solutions, though they rely heavily on handcrafted heuristics and expert knowledge. To address the gap, we propose **DRAGON**, a framework that transforms complex large COP solving into decomposition and reconstruction tasks guided by LLM agents. DRAGON first strategically identifies regions with high potential of improvement, decomposing large-scale COPs into context-manageable subproblems, and locally optimizes each subregion through reconstruction.

To concretely illustrate this idea, Figure 1 demonstrates an example of how the proposed Dragon improves TSP solution locally and globally. Given an initial global solution, the decomposition agent \mathcal{D} identifies nodes $\{4, 6, 7, 8\}$ (highlighted in gray) as a subproblem with high potential for further improvement, while the remaining nodes remain static and impose boundary constraints. During reconstruction, the suboptimal local segment (4-8-6-7) is locally optimized with LLM agents, leading to a better sub-solution

(4-6-7-8). Consequently, the improved local segment is integrated into the global solution, yielding a reduced tour length solution.

Overall, our contributions are threefold: (1) To the best of our knowledge, this is the first work to demonstrate that LLM agents can be effectively leveraged to directly generate high-quality solutions for large-scale COPs, opening new possibilities for LLM-driven optimization. (2) We propose DRAGON, a divide-and-conquer framework that dynamically decomposes large-scale COPs and subsequently refines compact subproblems by state passing between agents. (3) We empirically validate DRAGON on large-scale COPs benchmarks, demonstrating substantial improvements in solution quality and scalability compared to state-of-the-art LLM-based baselines. Our findings validate the feasibility of leveraging LLM agents for large-scale COPs that are prevalent in real-world applications.

2 RELATED WORK

LLMs for Combinatorial Optimization. Recent studies have increasingly examined the capability of LLMs to solve COPs by leveraging prompt engineering techniques. Among these efforts, a prominent direction involves using LLMs directly as solution generators, where carefully designed prompts and enriched input information guide the models to produce viable solutions. Early research by Wang et al. [37] provided evidence that LLMs could solve certain graph-based COPs, although this capability was strongly tied to the quality of the provided prompts. Subsequent work has sought to refine this process by incorporating contextual information. Examples include integrating graph structural and topological data [38], existing heuristic solutions [17], explicit relationships between solutions and objectives [41], and visual representations of problems or solutions [12, 16]. Another research pathway involves leveraging LLMs as components within structured algorithms or frameworks. For instance, Liu et al. [24] demonstrated the utility of LLMs in evolutionary computation by prompting them to perform essential algorithmic operations such as selection, crossover, and mutation. Similarly, Elhenawy et al. [13] deployed multiple LLMs as collaborative agents, each responsible for distinct roles such as initialization, critique, and evaluation within a predefined optimization pipeline. Despite these promising advancements, current capabilities for directly generating solutions via LLMs remain largely restricted to relatively small-scale problems, typically limited to instances such as TSP with fewer than 30 nodes. To circumvent this limitation, Iklassov et al. [17] introduced a decomposition approach wherein an LLM assesses problem complexity autonomously. If deemed difficult, the model recursively subdivides the problem into simpler, manageable subproblems. Nonetheless, its scalability remains limited.

Beyond direct solution generation, other studies have explored leveraging LLMs for heuristic design [23, 33, 42] and mathematical modeling [2, 20, 40]. The former aims to use LLMs to discover heuristics expressed in code that have potential to outperform those crafted by human experts, while the latter focuses on translating natural language problem descriptions into mathematical formulations compatible with traditional OR solvers. More recently, research has investigated training large language models for end-to-end combinatorial optimization, rather than relying solely on prompting paradigms [18, 19]. These directions fall outside the scope of this

work, and we refer interested readers to Da Ros et al. [11] for a comprehensive survey.

Large-Scale Combinatorial Optimization. Another research direction related to this work aiming to design metaheuristics for solving large-scale COPs, either with machine learning [21, 35] or through traditional methods [3, 34]. These approaches generally follow decomposition or divide-and-conquer principles. While they have shown promising results, their effectiveness often relies on problem-specific strategies (e.g., domain-specific decomposition rules), which limits their generality. In this work, we propose DRAGON, a general decomposition-reconstruction framework leveraging the semantic capabilities of LLMs. Unlike previous methods, DRAGON identifies suboptimal regions without explicit domain-specific rules and iteratively reconstructs globally consistent solutions. Our framework effectively addresses LLM context-length constraints, combining learned decomposition advantages with the generalization provided by LLM agents.

3 METHODOLOGY

DRAGON is a two-stage framework that enables LLM agents to effectively solve large-scale COPs via state passing communication. As illustrated in Figure 2, DRAGON iteratively alternates between two core tasks: Decomposition and Reconstruction. Starting from an initial solution generated by any fast heuristic, DRAGON progressively refines it by identifying subregions with high improvement potential and solving localized subproblems under explicit constraint awareness. In each iteration, the current solution is decomposed into manageable subproblems, locally optimized through reconstruction agents, and then reassembled into a globally improved solution. This hierarchical process unifies local and global optimization, allowing DRAGON to scale from small instances to complex large-scale COPs. The example workflow illustrated in Figure 1 is summarized in Algorithm 1, where implicit communication between agents occurs via solution state passing, and the subsequent sections detail each component of the framework.

Algorithm 1 DRAGON for Large-Scale COPs

```

Require: Metadata  $M$ , initial solution  $S_0$ , maximum time  $T_{\max}$ , rejection threshold
         $N$ 
Ensure: Improved solution  $S$ 
1:  $S \leftarrow S_0$                                      // Current solution
2:  $t \leftarrow 0$                                      // Time counter
3:  $r \leftarrow 0$                                      // Rejection counter
4: while  $t < T_{\max}$  and  $r < N$  do
5:    $(a, s) \leftarrow \mathcal{D}(M, S)$                    // Decomposition
6:    $(M', S', C) \leftarrow \text{Compress}(M, a, s)$ 
7:    $S'_{\text{new}} \leftarrow \mathcal{R}(M', S', C)$            // Reconstruction
8:   if  $\text{Accept}(S', S'_{\text{new}})$  then
9:      $S' \leftarrow S'_{\text{new}}$ 
10:     $S \leftarrow \text{Integration}(S', S)$ 
11:     $r \leftarrow 0$                                      // Reset rejection counter
12:  else
13:     $r \leftarrow r + 1$ 
14:  end if
15:   $t \leftarrow \text{Elapsed Time}()$                    // Reach running time limit.
16: end while
17: return  $S$ 

```

3.1 Framework Inputs and Solution Updates

DRAGON interacts with problem environment that contains two fundamental inputs: metadata M and the current solution S . Metadata M , represented as structured JSON, encodes essential problem-specific parameters, and the solution S is represented as an ordered sequence of elements, such as city indices for TSP or item identifiers for Knapsack, and is formatted in either JSON or XML, as illustrated in Figure 2(a).

Formally, given metadata M , the global solution at iteration i is obtained as follows:

$$S_i = \begin{cases} \text{Fast_Heuristic}(M), & i = 0 \\ \text{Integration}(S'_{i-1}, S_{i-1}), & i > 0 \\ S'_{i-1} = \mathcal{R}(\mathcal{D}(M, S_{i-1})), & i > 0 \end{cases} \quad (1)$$

Here, S'_{i-1} denotes the locally refined sub-solution from the previous iteration, identified by the decomposer \mathcal{D} and enhanced by the reconstructor \mathcal{R} (both detailed in subsequent sections). Integration involves simply concatenation and sorting operations, while specific implementation of `Fast_Heuristic` are provided in the experimental section. Furthermore, a new solution is conditionally accepted using a probabilistic criterion (assuming minimization):

$$\text{Accept}(S_1, S_2) = \min \left\{ 1, \exp \left(-\frac{f(S_2) - f(S_1)}{T} \right) \right\} \quad (2)$$

where f denotes the objective function and T is a temperature parameter controlling the acceptance probability. As shown in Algorithm 1, we substitute the current local solution S'_i and its \mathcal{R} processed version $S'_{\text{new},i}$ into Eq. 2 as S_1 and S_2 , respectively, and accepted solutions are then integrated back into the global solution to ensure consistency and feasibility. It is worth noting that even when the new local solution is worse i.e., $f(S'_{\text{new},i}) \geq f(S'_i)$, there remains a small chance of acceptance and integration, allowing DRAGON to occasionally accept inferior solutions, helping it escape local optima, promote exploration of the solution space, and maintain a balancing between exploitation and exploration.

Balancing exploitation (greedy improvement) and exploration (diversification) is critical to the performance of heuristic search methods. In many cases, domain experts must carefully design problem-specific strategies to achieve this balance, and the convergence rate of the solution gap can vary significantly depending on the designer's expertise. However, for large-scale COPs where analyzing the problem structure is extremely challenging and generalization across domains is difficult, we leverage LLM-based agents, which are well-suited for both exploitation and exploration, because they can exploit stored experiences from previous trials, while their generative and adaptive capabilities enable diverse solution proposals, supporting broader exploration of the solution space.

3.2 Decomposition for Large-Scale COPs

A central challenge in applying LLMs to large-scale COP decomposition lies in their limited capability to reason over complex global constraints. Although existing studies demonstrate the potential of LLMs in solving COPs [39, 41], their capability to accurately detect and isolate sub-problems suitable for local refinement within large-scale COPs remains largely unexplored. To this end, we propose a decomposition agent (\mathcal{D}) which leverages LLMs to strategically

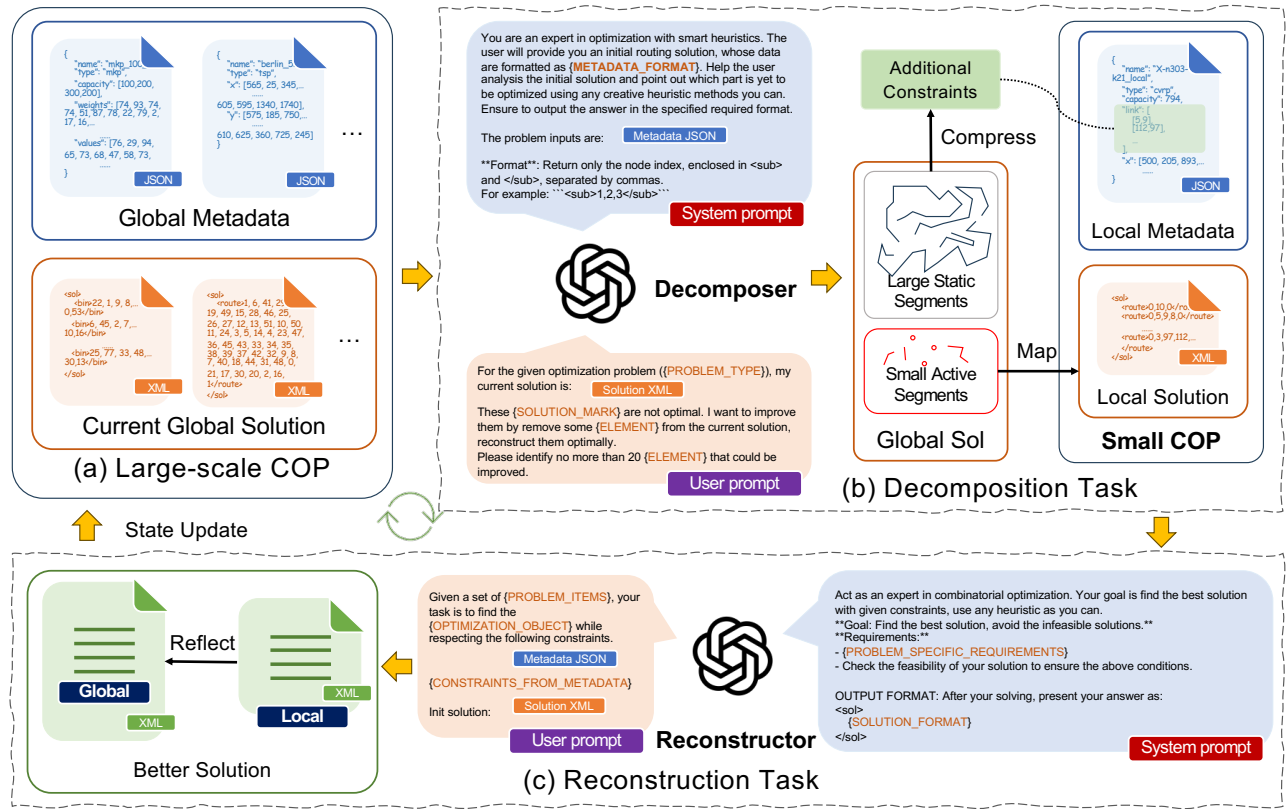


Figure 2: Overview of the state passing among agents in DRAGON framework. With (a) given COP data input and current global solution, the DRAGON pipeline process alternates between two key stages: (b) A decomposition step uses an LLM to split a large-scale COP into manageable active and static segments. These are compressed into a smaller subproblem; (c) A reconstruction step solves the reduced problem with additional constraints to yield a refined local solution. This is then reintegrated into the global solution.

partition COPs into smaller, manageable sub-problems for further refinement, rather than directly solving the entire COP. Specifically, the decomposer \mathcal{D} functions as a high-level planner, analyzing metadata M and the current solution S_i . It partitions the solution into *active segments* (a_i), which have substantial improvement potential, and *static segments* (s_i), which remain unchanged during the current iteration. Specifically, decomposition can be formulated as:

$$(a_i, s_i) = \mathcal{D}(M, S_i) \quad (3)$$

DRAGON demonstrates that well-designed prompts (illustrated in Figure 2(b) and Supplementary Materials (Prompt designs)) enable LLMs to effectively identify segments with significant potential for improvement while introducing additional constraints (C_i) to maintain feasibility and global consistency:

$$(M'_i, S'_i, C_i) = \text{Compress}(M, a_i, s_i) \quad (4)$$

where $M'_i \subseteq M$ denotes the subset of original metadata relevant only to the active segments. For example, in the TSP scenario illustrated in Figure 1, the decomposer identifies an active segment $a_i = \{4, 6, 7, 8\}$ and a static segment $s_i = [9, 0, 1, 2, 3, 5]$. The Compress step significantly reduces the size of the local data

$|M'_i| << |M|$, making it manageable to downstream agents. However, it will introduce extra specific constraints, which are a set of compressed representations of static segment s_i (e.g., enforce edge preservation like $(9, 5) \in C_i$).

3.3 Reconstruction with Constraint Integration

Recent studies [17, 24, 41] highlight the effectiveness of LLMs in solving small-scale COPs, typically with fewer than 30 decision variables. Building on this capability, our reconstruction agent (\mathcal{R}) is designed to solve compressed COP instances iteratively, derived from the decomposition stage.

Specifically, reconstructor \mathcal{R} utilizes localized metadata M'_i augmented with explicit constraints C_i to ensure global feasibility and consistency. Constraints C_i are explicitly integrated into natural language within the LLM prompt, with the formats varying by COP type. Formally, the reconstruction process is defined as:

$$S'_{\text{new},i} = \mathcal{R}(M'_i, S'_i, C_i) \quad (5)$$

where M'_i encapsulates localized metadata, and C_i encodes global consistency requirements derived from static segments s_i .

Note that the format and interpretation of constraints depend on the specific COP type. In routing problems such as TSP and CVRP,

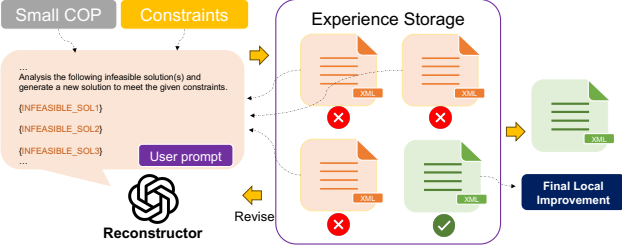


Figure 3: Constraint satisfaction in reconstruction is ensured via experience accumulation.

constraints typically enforce particular edge sequences to ensure route continuity, while in packing problems like MKP or BPP, constraints explicitly mandate item inclusion or exclusion. For instance, a constraint prompt for TSP may state: *“the following edges must be visited consecutively, with no additional points permitted between them.”* It is essential to maintain consistency between constraints and compressed metadata. For example, required edges (a, b) in CVRP represent condensed segments from the original route, with associated demands accurately reflecting the cumulative demands of intermediate nodes.

As illustrated in Figure 3, reconstruction agent utilizes iterative experience storage collected along previous trails to self-revise candidate solutions until all specified constraints are satisfied. The agent’s experience storage records all previous attempts, regardless of whether they result in feasible solutions or not, along with annotations on the type and cause of any constraint violations. This memory allows the agent to learn from past infeasible solutions, avoid repeating similar errors, and identify patterns within feasible solutions to guide future improvements. Through this process of iterative refinement, localized solutions are gradually adjusted to remain coherent and globally feasible. Extensive experiments detailed in the experimental section and Supplementary Materials demonstrate that, when guided by well-structured prompts and clearly defined constraints, LLM agents can consistently generate high-quality solutions to constrained subproblems.

4 EXPERIMENTS

4.1 Setup

4.1.1 Problem Descriptions. To evaluate the effectiveness and generalizability of the proposed DRAGON framework, we conduct experiments on four representative COPs across routing, packing and assignment domains:

- Traveling Salesman Problem (TSP): A classical combinatorial routing problem that seeks the shortest possible tour visiting each city exactly once and returning to the starting point.
- Capacitated Vehicle Routing Problem (CVRP): Extension of TSP with multiple vehicles and demand constraints. The goal is to minimize total travel distance while satisfying delivery demands.
- Bin Packing Problem (BPP): Classical combinatorial optimization problem where items of various sizes must be packed into a minimal number of fixed-capacity bins without exceeding their limits.

- Multiple Knapsack Problem (MKP): A generalization of the 0–1 knapsack problem involving multiple independent knapsacks. Unlike the multi-dimensional knapsack problem [9], where each item is constrained by several resource limits, the MKP aims to maximize the total value by optimally assigning items to knapsacks without exceeding their individual capacities.

4.1.2 Datasets.

- **TSP** We use 77 benchmark instances from TSPLIB [31] of the EUC_2D type, with sizes ranging from 50 to 20k nodes, covering a broad range of scales and spatial layouts. **Oracle:** optimal values or lower bounds reported in [31].
- **CVRP** We select subsets of 19 instances from CVRPLIB, including both X-type [36] (up to 1000 nodes) and larger XML-type instances [30] distribution, which was synthesized at large scale (up to 5k nodes) by [44]. **Oracle:** optimal values or lower bounds reported in [36, 44].
- **BPP** We adopt instances from FunSearch [33] and EoH [23] of all Weibull-5k, which is reflecting real-world scheduling and allocation scenarios. **Oracle:** L2 lower bounds determined by [33].
- **MKP** Following Google OR-Tools guidelines [28], we generate 10 synthetic instances by with knapsack capacities uniformly sampled from $U(100, 500)$, using 10 to 100 knapsacks. Item values and weights drawn uniformly from $U(1, 100)$. All instances will be released in supplementary JSON files. **Oracle:** optimal values or uppers bound searched by solver.

4.1.3 Implementation Details. We evaluate our framework using four representative LLMs accessed via API: two general-purpose models, OpenAI’s gpt-4o and gpt-4.1, and two reasoning-specialized models, OpenAI’s o3 and DeepSeek’s r1. Due to time and cost constraints, we limit our experiments to these models. Prompting strategies for each stage of DRAGON are illustrated in Figure 2, with complete prompt templates provided in the Appendix (Prompt designs). We adopt simple global solution initialization algorithms to each problem: 1) Random Insertion [5] for TSP, 2) Greedy Nearest Neighbor heuristic [26] for CVRP, and 3) First-Fit Decreasing [6] for both BPP and MKP. For comparative evaluation, we implement OR-Tools [28] solvers as: CVRP is solved via the routing model [15] with *Guided_Local_Search*¹ as the metaheuristic, while BPP uses the CP-SAT [27]. All experiments run on an Ubuntu 20.04 server with an Intel Core i9-10900X (20 cores at 4.6 GHz) without GPU. For detailed prompt designs used in the decomposition and reconstruction processes, please refer to the Supplementary Materials.

4.1.4 Feasibility check. Feasibility checking for solutions obtained by any method is straightforward. We implement a checker based on the inherent constraints of each COP type. If a solution is found to be infeasible, it is stored in the agent’s memory along with comments explaining the reason for infeasibility. This feedback helps the agent avoid repeating the same mistakes, thereby reducing search time and accelerating convergence to feasible solutions. In the results presented later, we denote an infeasible solution as “infe” and use

¹https://developers.google.com/optimization/routing/routing_options

Table 1: Average optimality gap (%) on routing problems using subsets from TSPLIB (EUC_2D) and CVRPLIB (Set X/XML).

Method		TSPLIB (EUC_2D)					
(size, k #)	0.05-0.5 42	0.5-1 6	1-2 15	2-5 7	5-20 7	All 77	
OPRO	inf	inf	inf	inf	inf	inf	
SGE	infe	infe	infe	infe	infe	infe	
LMEA	820.30	2279.35	3578.21	inf	inf	inf	
ReEvo(c)	12.69	16.43	17.01	inf	inf	inf	
ReEvo(a)	8.17	16.61	18.23	21.20	18.62	13.10	
DRAGON	9.74	11.24	15.24	19.37	15.42	12.24	
Method		CVRPLIB (X/XML)					
(size, k #)	0.1-0.2 2	0.2-0.5 3	0.5-1 5	1-2 3	2-5 3	≥5 3	All 19
OR-Tools	inf	inf	inf	inf	inf	inf	
ReEvo(a)	21.49	19.27	29.44	25.39	22.00	11.24	24.17
DRAGON	25.56	29.35	26.73	15.51	15.48	6.45	20.15

“inf” to indicate cases where the solving time exceeds the given time limit T_{\max} .

4.1.5 Metrics. We evaluate performance using four metrics: (1) Optimality Gap defined as $Gap = \frac{|v-v^*|}{v^*} \times 100\%$, where v and v^* are the objective value and the optimal value, respectively; (2) Running Time (seconds); (3) Input/Output Token Counts; and (4) Number of API Calls. All experiments use consistent settings with a 1-hour time limit $T_{\max} = 3600$ and early stopping after $N = 5$ consecutive non-improving iterations.

4.2 Performance Evaluation

To evaluate performance on large-scale routing problems (TSP and CVRP), Table 1 presents the average optimality gap (%) across different instance size groups, comparing DRAGON with existing LLM-based solvers, including prompt-based methods (OPRO [41], SGE [17]) and code-generation approaches (LMEA [24], ReEvo [42], with ReEvo(a) using Ant Colony Optimization (ACO) and ReEvo(c) employing a constructive heuristic). To ensure a fair comparison, all LLM-based methods use gpt-4o, with token usage and inference time recorded. Instances are grouped by node size for conciseness, and detailed results are listed in Supplementary Materials.

OPRO fails to return valid solutions for all groups, as some hard instances in groups exceed the runtime limit, resulting in an infinite gap inf. SGE consistently produces infeasible solutions (infe), likely because it lacks explicit feasibility checks, since its original design is for small problems (under 30 nodes). LMEA handles slightly larger instances but exhibits high gaps and fails beyond 2k-node due to prompt length limits and generation timeouts.

As shown in Figure 4, results on TSPLIB reveal that SGE is excluded due to infeasible solutions, while OPRO is omitted as “inf” that no solution found due to its slow inference time across all groups. LMEA is able to solve up to medium-sized instances but exhibits relatively large optimality gaps. ReEvo(c) achieves

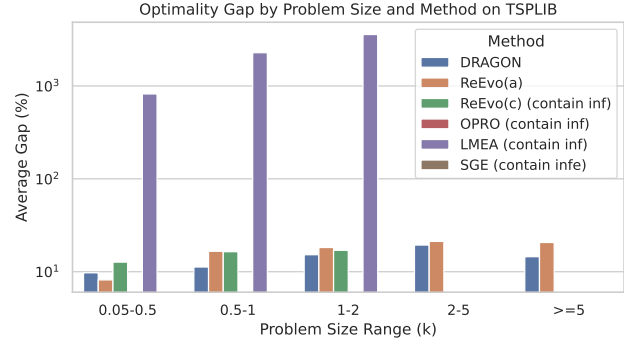


Figure 4: Average Optimality Gap (%) (log scale) across problem size groups for different methods on TSPLIB.

strong results up to the medium-size group, whereas ReEvo(a) excels on smaller instances. Although DRAGON does not outperform across every group, it demonstrates clear superiority on larger-scale problems, benefiting from its task allocation mechanism, where decomposition and reconstruction collaborate effectively.

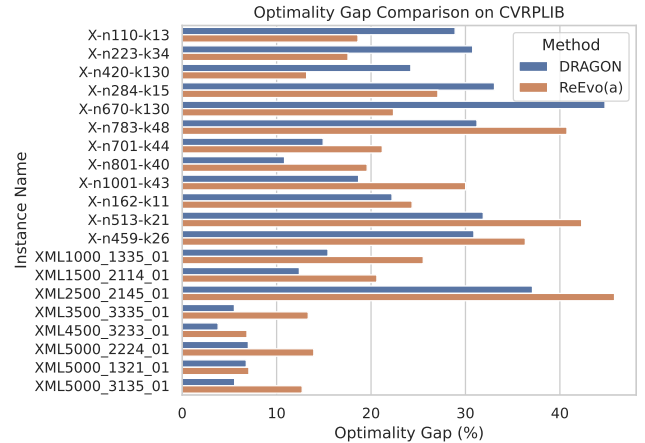


Figure 5: Optimality Gap (%) for different methods on CVRPLIB.

Figure 5 presents the methods capable of obtaining feasible solutions for CVRP instances. As CVRP is inherently more complex than TSP, DRAGON outperforms ReEvo(a) primarily on large-scale problems, where its decomposition-reconstruction mechanism demonstrates greater advantages.

These findings highlight a major limitation of pure prompt-based methods: while capable of solving small to medium-scale COPs, their performance degrades significantly as problem size increases. This is mainly due to long context lengths and high decoding cost—making token-by-token generation unstable when encountering large input loads. Code-generation methods like ReEvo improve scalability. We tested ReEvo’s released heuristic code, including both constructive (ReEvo(c)) and ACO-enhanced (ReEvo(a)) variants. On TSPLIB, DRAGON consistently outperforms ReEvo(c)

Table 2: Domain expertise levels across decomposition-reconstruction strategy combinations. Each cell shows expertise needed: \times (none), \checkmark (some), $\checkmark\checkmark$ (extensive) for decomposition and reconstruction, respectively.

Decomposition	Reconstruction		
	Heuristic	Solver	LLM
Random	(\times , \checkmark)	(\times , $\checkmark\checkmark$)	(\times , \times)
Heuristic	(\checkmark , \checkmark)	(\checkmark , $\checkmark\checkmark$)	(\checkmark , \times)
LLM	(\times , \checkmark)	(\times , $\checkmark\checkmark$)	(\times , \times)

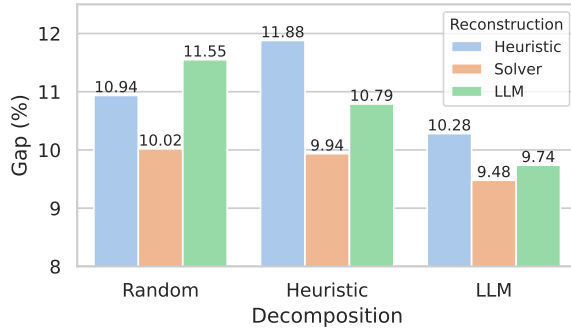


Figure 6: Ablation study of DRAGON across 9 decomposition-reconstruction combinations as listed in Table 2. Bars show the optimality gap (%) compared to the known optimal value on a TSPLIB subset.

across all size groups and also surpasses ReEvo(a) on all groups beyond 500, and achieving an average gap reduction of 0.86%. On CVRPLIB, where OR-Tools fails to find feasible solutions within time limit, DRAGON leads around 3.98% lower gaps than ReEvo(a) on all cases. Overall, DRAGON demonstrates the best average performance across routing benchmarks, validating its effectiveness and scalability.

4.3 Ablation Study

4.3.1 Strategies for Decomposition and Reconstruction. DRAGON supports configurable strategies for each task, allowing us to evaluate the impact of different implementations. Table 2 presents a 3×3 combination of decomposition and reconstruction strategies, along with the domain expertise required for each pair, offering insight into their implementation difficulty. For decomposition, “Random” selects elements arbitrarily, “Heuristic” applies domain-specific rules, and “LLM” leverages large language models. Similarly for strategies in reconstruction, the only new word “Solver” refers to implement general purpose solver. Figure 6 shows the performance of DRAGON on a TSPLIB subset using these nine combinations.

Among reconstruction strategies, the solver-based approach achieves the best performance by optimally solving small size local COPs. However, this method has key drawbacks: (1) in routing problems for example, enforcing must-visit edges via zero distances with penalty trick may not lead to the constraint satisfied outcomes, and

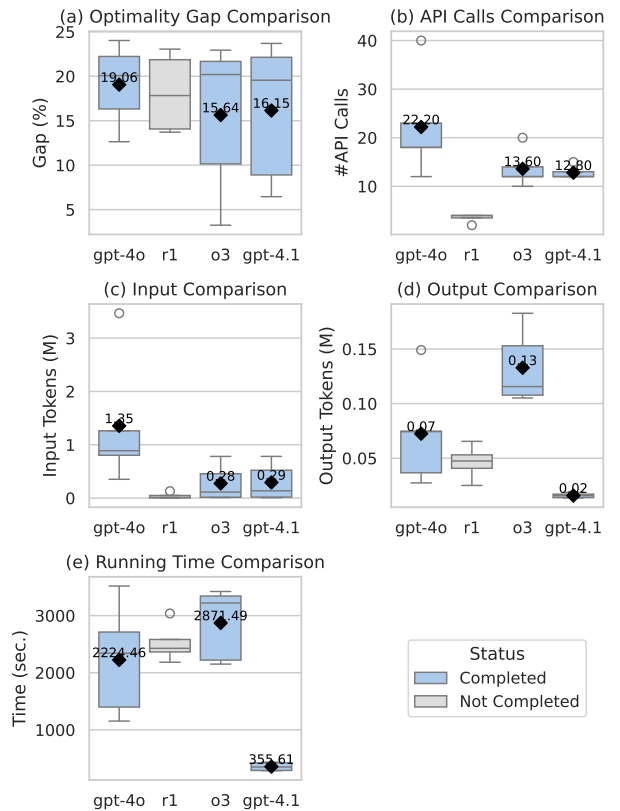


Figure 7: Comparison of different LLM models by: (a) optimality gap, (b) number of API calls, (c) input tokens, (d) output tokens, (e) running time. We evaluate general-purpose models (gpt-4o, gpt-4.1) and reasoning-oriented models (o3, r1). Gray bars indicate incomplete results due to token limit violations on the largest instance.

(2) encoding custom constraints across diverse COPs requires substantial domain expertise, as reflected in Table 2. Despite requiring the most domain knowledge, the “Heuristic×Solver” combination does not yield the best results. In contrast, our DRAGON pipeline “LLM×LLM” outperforms it, highlighting the effectiveness of LLM-based decomposition agent in capturing promising substructures. Notably, reconstruction agent offers ease of implementation and integrates naturally with decomposition agent. Hence, DRAGON strikes a strong balance between performance and usability, making it practical.

4.3.2 Impact of LLM backbones. As shown in Figure 7, we evaluate the impact of different LLM backbones within the DRAGON framework, including general-purpose models (OpenAI gpt-4o, gpt-4.1) and reasoning models (OpenAI o3, DeepSeek r1). Due to cost considerations, we do not evaluate all TSPLIB instances. As r1 exceeds the model’s input token limit of 65,536 on instances larger than 10k nodes, it fails to produce responses in the largest case (listed in Appendix (Experiment results)).

Table 3: Average optimality gap (%) w.r.t. L2 lower bound and inference time (sec.) on the Weibull-5K dataset.

Method	ReEvo(a)	FunSearch	EoH	EoH expert	Ours
Gap (%) ↓	3.46	0.69	0.66	0.55	0.33
Time (sec.) ↓	56.677	2.292	-	-	487.873

While o3 achieves the lowest average optimality gap, it incurs extremely high output token counts. Given that OpenAI’s API typically prices output tokens at 4 times the rate of input tokens, this leads to significantly higher costs and longer inference time. r1 exhibits a relatively low number of API calls, suggesting that each call takes longer—likely due to more intensive reasoning per iteration. Considering the trade-off between objective quality, inference speed, and token efficiency, gpt-4.1 achieves the best overall balance and emerges as the current most practical choice.

4.4 Generalization Case Study

To assess the robustness of DRAGON, we evaluate its performance across more domains, it highlights the method’s ability to generalization for the subsequent results.

4.4.1 Bin Packing Problem. In addition to routing problems, we evaluate DRAGON on the packing domain. As shown in Table 3, DRAGON consistently outperforms ReEvo(a), FunSearch, EoH, and EoH expert on the Weibull-5K dataset. We omit OR-Tools solvers (both MP and CP-SAT backends) as they failed to produce feasible solutions before timeouts.

Compared to routing, packing problems are generally easier for LLMs to reason about due to their more intuitive and straightforward constraints. For example, merging static segments (s) into packed items requires less complex reasoning, allowing DRAGON to scale more effectively to larger instances. Results for EoH and EoH expert are reported directly from [23], where running time was not provided. While DRAGON achieves the lowest optimality gap, it is slower than code-generation based methods. However, code-generation approaches come with high API costs and substantial time and resources to evolve or fine-tune high-quality heuristic functions. These overheads are not captured in current comparison. Each paradigm has its strengths. For large batches of similar instances, code-generation methods are effective as the learned heuristic can be reused across the dataset. In contrast, prompt-based approaches like DRAGON are better suited for dynamic environments where instance structures vary, offering flexibility without the need for retraining or code evolution.

4.4.2 Multiple Knapsack Problem. We compare DRAGON with the CP-SAT on a series of synthetic MKP instances. Each instance is named using the format $\text{mfp_}n_{\text{item}}\text{-}n_{\text{knapsack}}$, where the decision space grows as $n_{\text{item}} \times n_{\text{knapsack}}$, hence the maximum of decision size here is around 3M.

As shown in Figure 8, CP-SAT typically achieves lower optimality gaps and can even find optimal solutions when the instance size is manageable. However, its performance starts to degrade on larger instances, evident from the largest case, where the gap spikes to around 3% and it hits the time limit. DRAGON performs favorably

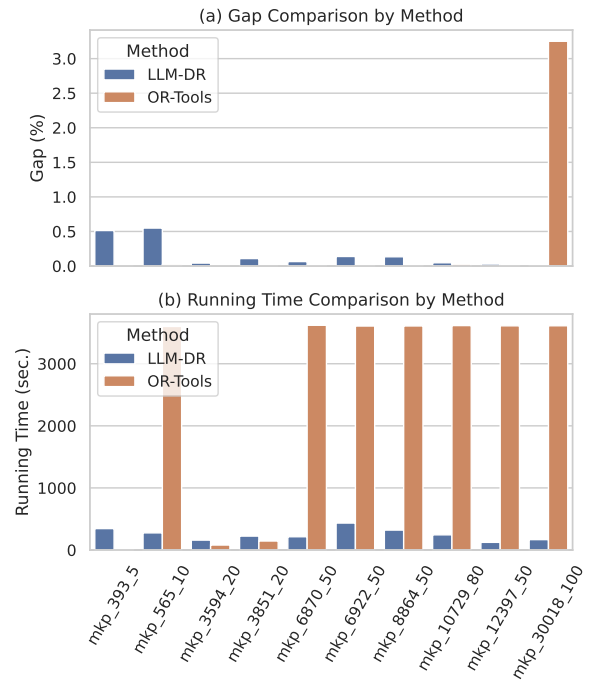


Figure 8: Comparison on synthetic Multiple Knapsack Problem instances between DRAGON and OR-Tools (CP-SAT).

across all instances. While its gap is generally slightly higher than CP-SAT on small cases, it remains consistently below 0.5%, even on large-scale instances. In terms of trade-offs between performance and efficiency, DRAGON offers strong scalability and competitive quality, delivering high-quality solutions within reasonable reasoning time, making it highly effective for large-scale MKPs where traditional solvers may struggle.

4.5 Limitations and Future Directions

While DRAGON demonstrates strong potential in solving large-scale COPs, several limitations remain to be addressed. The quality of the reconstructed global solution is sensitive to both the decomposition strategy and the prompt formulation. Inappropriate segmentation or poorly structured prompts may lead to suboptimal or degenerated solutions, emphasizing the need for more robust and adaptive decomposition mechanisms. Moreover, the iterative nature of DRAGON introduces substantial computational overhead due to the large context required during each divide-and-conquer cycle, resulting in extended runtime. Although the current pipeline may not be efficient for small-scale problems, it proves particularly advantageous for super large-scale scenarios where traditional solvers and other learning-based methods struggle to deliver feasible or high-quality solutions across all testing tasks.

DRAGON also demonstrates that purely language-based agents can effectively address large-scale COPs, outperforming other prompt-based or code-generation-based approaches. Additionally, incorporating external optimization tools such as OR-Tools within the reconstruction stage enhances local refinement. However, the use of

such tools often demands additional modeling expertise, especially for non-standard constrained sub-problem settings.

In the on-going work, we are integrating more external tools to automatically model customized constraints not only within the reconstruction agent but also into the decomposition process, with the goal of further reducing runtime and API costs while maintaining or improving solution quality. We also envision introducing a central coordination agent to better manage the interaction among decomposition and reconstruction agents, thereby improving the overall consistency and efficiency of the optimization process.

5 CONCLUSION

This paper presents DRAGON, a novel framework that leverages LLM agents to solve large-scale COPs via an iterative decomposition reconstruction process inspired by divide-and-conquer. Experiments across diverse COP domains (e.g., routing and packing) show that DRAGON consistently achieves strong performance, especially on extreme large instances where traditional solvers or basic prompt-based methods often fail due to scalability or timeouts. By decomposing complex problems into context manageable subproblems, DRAGON enables LLMs to reason effectively over intricate structures, identifying promising regions, and reconstructing feasible global solutions. This training-free, modular, and solver-agnostic approach supports flexible constraint handling and adapts easily to diverse COPs without specialized algorithm design. Although not optimized for speed, DRAGON avoids expensive code search and offers a strong balance between solution quality, adaptability, and cost, making it particularly well-suited for dynamic and large-scale settings. Future work will focus on enhancing decomposition strategies, improving prompt robustness, and integrating hybrid solvers to explore promising regions more efficiently.

Overall, DRAGON establishes a solid foundation toward general-purpose, interpretable, and scalable LLM-based optimization.

ACKNOWLEDGMENTS

This research/project is supported by the National Research Foundation, Singapore under its AI Singapore Programme (AISG Award No: AISG3-RPGV-2025-017, AISG3-RP-2025-036-USNSF).

REFERENCES

- [1] Josh Achiam, Steven Adler, Sandhini Agarwal, Lama Ahmad, Ilge Akkaya, Florencia Leoni Aleman, Diogo Almeida, Janko Altenschmidt, Sam Altman, Shyamal Anadkat, et al. 2024. Gpt-4 technical report. *arXiv preprint arXiv:2303.08774* [cs.CL]
- [2] Ali AhmadiTeshnizi, Wenzhi Gao, and Madeleine Udell. 2024. OptiMUS: Scalable Optimization Modeling with (MI)LP Solvers and Large Language Models. In *International Conference on Machine Learning (Proceedings of Machine Learning Research, Vol. 235)*, Ruslan Salakhutdinov, Zico Kolter, Katherine Heller, Adrian Weller, Nuria Oliver, Jonathan Scarlett, and Felix Berkenkamp (Eds.). PMLR, 577–596.
- [3] Florian Arnold, Michel Gendreau, and Kenneth Sørensen. 2019. Efficiently solving very large-scale routing problems. *Computers & operations research* 107 (2019), 32–42.
- [4] Giorgio Ausiello, Pierluigi Crescenzi, Giorgio Gambosi, Viggo Kann, Alberto Marchetti-Spaccamela, and Marco Protasi. 2012. *Complexity and approximation: Combinatorial optimization problems and their approximability properties*. Springer Science & Business Media.
- [5] Yossi Azar. 1994. Lower bounds for insertion methods for TSP. *Combinatorics, Probability and Computing* 3, 3 (1994), 285–292.
- [6] Brenda S Baker. 1985. A new proof for the first-fit decreasing bin-packing algorithm. *Journal of Algorithms* 6, 1 (1985), 49–70.
- [7] Yoshua Bengio, Andrea Lodi, and Antoine Prouvost. 2021. Machine learning for combinatorial optimization: a methodological tour d’horizon. *European Journal of Operational Research* 290, 2 (2021), 405–421. <https://doi.org/10.1016/j.ejor.2020.07.063>
- [8] Tom Brown, Benjamin Mann, Nick Ryder, Melanie Subbiah, Jared D Kaplan, Prafulla Dhariwal, Arvind Neelakantan, Pranav Shyam, Girish Sastry, Amanda Askell, et al. 2020. Language models are few-shot learners. *Advances in neural information processing systems* 33 (2020), 1877–1901.
- [9] Valentina Cacchiani, Manuel Iori, Alberto Locatelli, and Silvano Martello. 2022. Knapsack Problems – An Overview of Recent Advances. Part II: Multiple, Multidimensional, and Quadratic Knapsack Problems. *Computers & Operations Research* 143 (2022), 105693. <https://doi.org/10.1016/j.cor.2021.105693>
- [10] Aakanksha Chowdhery, Sharan Narang, Jacob Devlin, Maarten Bosma, Gaurav Mishra, Adam Roberts, Paul Barham, Hyung Won Chung, Charles Sutton, Sebastian Gehrmann, et al. 2023. Palm: Scaling language modeling with pathways. *Journal of Machine Learning Research* 24, 240 (2023), 1–113.
- [11] Francesca Da Ros, Michael Soprano, Luca Di Gaspero, and Kevin Roitero. 2025. Large Language Models for Combinatorial Optimization: A Systematic Review. *arXiv preprint arXiv:2507.03637* (2025).
- [12] Mohammed Elhenawy, Ahmed Abdelhay, Taqwa I Alhadidi, Huthaifa I Ashqar, Shadi Jaradat, Ahmed Jaber, Sébastien Glaser, and Andry Rakotonirainy. 2024. Eyeballing Combinatorial Problems: A Case Study of Using Multimodal Large Language Models to Solve Traveling Salesman Problems. *arXiv preprint arXiv:2406.06865* (2024), 341–355.
- [13] Mohammed Elhenawy, Ahmad Abutahoun, Taqwa I Alhadidi, Ahmed Jaber, Huthaifa I Ashqar, Shadi Jaradat, Ahmed Abdelhay, Sébastien Glaser, and Andry Rakotonirainy. 2024. Visual Reasoning and Multi-Agent Approach in Multimodal Large Language Models (MLLMs): Solving TSP and mTSP Combinatorial Challenges. *Machine Learning and Knowledge Extraction* 6, 3 (2024), 1894–1920.
- [14] Shaodi Feng, Zhuoyi Lin, Jianan Zhou, Cong Zhang, Jingwen Li, Kuan-Wen Chen, Senthilnath Jayavelu, and Yew-Soon Ong. 2025. Lifelong Learner: Discovering Versatile Neural Solvers for Vehicle Routing Problems. *arXiv preprint arXiv:2508.11679* (2025).
- [15] Vincent Furnon and Laurent Perron. 2025. OR-Tools Routing Library. <https://developers.google.com/optimization/routing/>. Version 9.12, Google.
- [16] Yuxiao Huang, Wenjie Zhang, Liang Feng, Xingyu Wu, and Kay Chen Tan. 2024. How multimodal integration boost the performance of llm for optimization: Case study on capacitated vehicle routing problems. *arXiv preprint arXiv:2403.01757* (2024).
- [17] Zangir Iklassov, Yali Du, Farkhad Akimov, and Martin Takac. 2024. Self-Guiding Exploration for Combinatorial Problems. *Advances in Neural Information Processing Systems* (2024).
- [18] Xia Jiang, Yaxin Wu, Minshuo Li, Zhiguang Cao, and Yingqian Zhang. 2025. Large Language Models as End-to-end Combinatorial Optimization Solvers. In *The Thirty-ninth Annual Conference on Neural Information Processing Systems*.
- [19] Xia Jiang, Yaxin Wu, Yuan Wang, and Yingqian Zhang. 2024. Bridging Large Language Models and Optimization: A Unified Framework for Text-attributed Combinatorial Optimization. *arXiv preprint arXiv:2408.12214* (2024).
- [20] Xia Jiang, Yaxin Wu, Chenhao Zhang, and Yingqian Zhang. 2025. DRoC: Elevating large language models for complex vehicle routing via decomposed retrieval of constraints. In *International Conference on Learning Representations*.
- [21] Sirui Li, Zhongxia Yan, and Cathy Wu. 2021. Learning to delegate for large-scale vehicle routing. In *Advances in Neural Information Processing Systems*, Vol. 34, 26198–26211.
- [22] Zhuoyi Lin, Yaxin Wu, Bangjian Zhou, Zhiguang Cao, Wen Song, Yingqian Zhang, and Senthilnath Jayavelu. 2024. Cross-problem learning for solving vehicle routing problems. In *Proceedings of the Thirty-Third International Joint Conference on Artificial Intelligence*. 6958–6966.
- [23] Fei Liu, Xialiang Tong, Mingxuan Yuan, Xi Lin, Fu Luo, Zhenkun Wang, Zhichao Lu, and Qingfu Zhang. 2024. Evolution of heuristics: towards efficient automatic algorithm design using large language model. In *Proceedings of the 41st International Conference on Machine Learning (Vienna, Austria) (ICML ’24)*. JMLR.org, Article 1304, 23 pages.
- [24] Shengcui Liu, Caishun Chen, Xinghua Qu, Ke Tang, and Yew-Soon Ong. 2024. Large language models as evolutionary optimizers. In *2024 IEEE Congress on Evolutionary Computation (CEC)*. IEEE, 1–8.
- [25] Yining Ma, Zhiguang Cao, and Yeow Meng Chee. 2023. Learning to search feasible and infeasible regions of routing problems with flexible neural k-opt. *Advances in Neural Information Processing Systems* 36 (2023), 49555–49578.
- [26] Mazin Abed Mohammed, Mohd Khanapi Abd Ghani, Raed Ibraheem Hamed, Salama A Mostafa, Dheyaa Ahmed Ibrahim, Humam Khaled Jameel, and Ahmed Hamed Alallah. 2017. Solving vehicle routing problem by using improved K-nearest neighbor algorithm for best solution. *Journal of Computational Science* 21 (2017), 232–240.
- [27] Laurent Perron and Frédéric Didier. 2025. CP-SAT Solver. https://developers.google.com/optimization/cp_cp_solver/. Version 9.12, Google.
- [28] Laurent Perron and Vincent Furnon. 2025. OR-Tools. <https://developers.google.com/optimization/>. Version 9.12, Google.

[29] David Pisinger and Stefan Ropke. 2018. Large neighborhood search. In *Handbook of metaheuristics*. Springer, 99–127.

[30] Eduardo Queiroga, Ruslan Sadykov, Eduardo Uchoa, and Thibaut Vidal. 2022. 10,000 optimal CVRP solutions for testing machine learning based heuristics. In *AAAI-22 Workshop on Machine Learning for Operations Research (ML4OR)*. <https://openreview.net/forum?id=yHiMXKN6nTl>

[31] Gerhard Reinelt. 1991. TSPLIB—A traveling salesman problem library. *ORSA journal on computing* 3, 4 (1991), 376–384.

[32] Nizar Rokbani, Raghvendra Kumar, Ajith Abraham, Adel M Alimi, Hoang Viet Long, Ishaani Priyadarshini, and Le Hoang Son. 2021. Bi-heuristic ant colony optimization-based approaches for traveling salesman problem. *Soft Computing* 25, 5 (2021), 3775–3794.

[33] Bernardino Romera-Paredes, Mohammadamin Barekatain, Alexander Novikov, Matej Balog, M Pawan Kumar, Emilien Dupont, Francisco JR Ruiz, Jordan S Ellenberg, Pengming Wang, Omar Fawzi, et al. 2024. Mathematical discoveries from program search with large language models. *Nature* 625, 7995 (2024), 468–475.

[34] Paul Shaw. 1998. Using constraint programming and local search methods to solve vehicle routing problems. In *International conference on principles and practice of constraint programming*. Springer, 417–431.

[35] Zhiqing Sun and Yiming Yang. 2023. DIFUSCO: Graph-based Diffusion Solvers for Combinatorial Optimization. In *Advances in Neural Information Processing Systems*.

[36] Eduardo Uchoa, Diego Pecin, Artur Pessoa, Marcus Poggi, Thibaut Vidal, and Anand Subramanian. 2017. New Benchmark Instances for the Capacitated Vehicle Routing Problem. *European Journal of Operational Research* 257, 3 (2017), 845–858. <https://doi.org/10.1016/j.ejor.2016.08.012>

[37] Heng Wang, Shangbin Feng, Tianxing He, Zhaoxuan Tan, Xiaochuang Han, and Yulia Tsvetkov. 2024. Can language models solve graph problems in natural language? *Advances in Neural Information Processing Systems* 36 (2024).

[38] Segev Wasserkrug, Leonard Boussioux, Dick den Hertog, Farzaneh Mirzazadeh, Ilker Birbil, Jannis Kurtz, and Donato Maragno. 2024. From Large Language Models and Optimization to Decision Optimization CoPilot: A Research Manifesto. *arXiv preprint arXiv:2402.16269* (2024).

[39] Michael Wilson, Jackson Petty, and Robert Frank. 2023. How Abstract Is Linguistic Generalization in Large Language Models? Experiments with Argument Structure. *Transactions of the Association for Computational Linguistics* 11 (Nov. 2023), 1377–1395. https://doi.org/10.1162/tacl_a_00608

[40] Ziyang Xiao, Dongxiang Zhang, Yangjun Wu, Lilin Xu, Yuan Jessica Wang, Xiongwei Han, Xiaojin Fu, Tao Zhong, Jia Zeng, Mingli Song, et al. 2023. Chain-of-Experts: When LLMs Meet Complex Operations Research Problems. In *International Conference on Learning Representations*.

[41] Chengrun Yang, Xuezhi Wang, Yifeng Lu, Hanxiao Liu, Quoc V Le, Denny Zhou, and Xinyun Chen. 2024. Large Language Models as Optimizers. In *International Conference on Learning Representations*.

[42] Haoran Ye, Jiarui Wang, Zhiguang Cao, Federico Berto, Chuanbo Hua, Haeyeon Kim, Jinkyoo Park, and Guojie Song. 2025. ReEvo: large language models as hyper-heuristics with reflective evolution. In *Proceedings of the 38th International Conference on Neural Information Processing Systems* (Vancouver, BC, Canada) (NIPS '24). Curran Associates Inc., Red Hook, NY, USA, Article 1381, 38 pages.

[43] Jie Zhao, Tao Wen, and Kang Hao Cheong. 2025. Can Large Language Models Be Trusted as Evolutionary Optimizers for Network-Structured Combinatorial Problems? *arXiv preprint arXiv:2501.15081* (2025).

[44] Jianan Zhou, Yaxin Wu, Wen Song, Zhiguang Cao, and Jie Zhang. 2023. Towards omni-generalizable neural methods for vehicle routing problems. In *Proceedings of the 40th International Conference on Machine Learning* (Honolulu, Hawaii, USA) (ICML '23). JMLR.org, Article 1803, 21 pages.

[45] Jianghan Zhu, Yaxin Wu, Zhuoyi Lin, Zhengyuan Zhang, Haiyan Yin, Zhiguang Cao, Senthilnath Jayavelu, and Xiaoli Li. 2025. Bridging Synthetic and Real Routing Problems via LLM-Guided Instance Generation and Progressive Adaptation. In *The 40th Annual AAAI Conference on Artificial Intelligence*.

A PROMPT DESIGNS

A.1 General DRAGON Prompts

To implement DRAGON, we detail the design of the prompts used by the framework, which consists of two main agents: the **Decomposer** and the **Reconstructor**. These LLM prompts are designed to be general-purpose and adaptable across various combinatorial optimization problems (COPs). They contain placeholders that should be customized based on the specific COP being addressed.

A.1.1 Decomposer’s System Prompt.

Decomposer System Prompt

You are an expert in optimization with smart heuristics. The user will provide you an initial solution, whose data are formatted as `{METADATA_FORMAT}`. Help the user analysis the initial solution and point out which part is yet to be optimized using any creative heuristic methods you can. Ensure to output the answer in the specified required format.

The problem inputs are:

`{INPUT_DATA}`

****Format**:** Return only the node index, enclosed in `_{` and `}`, separated by commas.

For example: `_{1,2,3}`

The placeholders above should be filled as follows:

- `METADATA_FORMAT`: A list of key-value pairs describing the structure of the solution input.
- `INPUT_DATA`: The actual raw input data to be passed to the LLM.

To align with our implementation, we recommend structuring the input data in a standardized JSON format, as illustrated in Table A1. Value types in the JSON schema are:

Table A1: Required keys in JSON format for different COPs. ✓ indicates mandatory fields, while ✓ marks optional fields that are applicable in routing problems with additional constraints.

Key	TSP	CVRP	BPP	MKP
“name”	✓	✓	✓	✓
“type”	✓	✓	✓	✓
“num”	✓	✓	✓	✓
“depot”		✓		
“x”	✓	✓		
“y”	✓	✓		
“weights”			✓	✓
“values”				✓
“capacity”		✓	✓	✓
“demand”		✓		
“link”	✓	✓		

- **String** (e.g., “name”, “type”),
- **Integer** (e.g., “depot” for CVRP, “capacity” for BPP, “num” refer to node size for TSP/CVRP and item size for BPP/MKP),
- **List of integers** (e.g., “x”, “y” for routing, “demand”, “capacity” for MKP).

For example of CVRP metadata:

Example JSON for CVRP

```
{
  "name": "CVRP-Example-001",
  "type": "cvrp",
  "num": 6,
  "depot": 0,
  "x": [50, 20, 40, 60, 80, 30],
  "y": [50, 70, 60, 40, 30, 90],
  "capacity": 100,
  "demand": [0, 10, 20, 30, 25, 15],
  "link": [
    [0, 5],
    [4, 2]
  ]
}
```

Decomposer's User Prompt:

Decomposer User Prompt

For the given optimization problem ({PROBLEM_TYPE}), my current solution is:

{SOLUTION}

These {SOLUTION_MARK} are not optimal. I want to improve them by remove some {ELEMENT} from the current solution, reconstruct them optimally. Please identify no more than {NUM} {ELEMENT} that could be improved.

Here's how to define the placeholders:

- PROBLEM_TYPE: Set as “tsp”, “cvrp”, “bpp”, or “mfp”.
- SOLUTION: The current solution in a structured format (e.g., XML or JSON). For CVRP, the XML looks like:

Example XML for CVRP

```
<sol>
  <route>0,2,3,0</route>
  <route>0,1,5,4,0</route>
</sol>
```

Table A2: Mapping of user prompt placeholders for COPs.

Placeholder	TSP	CVRP	BPP	MKP
SOLUTION_MARK	“route”	“route”	“pack”	“pack”
ELEMENT	“node”	“node”	“item”	“item”

We set NUM = 20 in all experiments. We recommend not exceeding 50, as the identified elements will be passed to the reconstructor, which may face difficulty handling larger inputs.

A.1.2 Reconstructor's System Prompt

Reconstructor System Prompt

Act as an expert in combinatorial optimization. Your goal is find the best solution with given constraints, use any heuristic as you can.

Goal: Find the best solution, avoid the infeasible solutions.

Requirements:

- {PROBLEM_SPECIFIC_REQUIREMENTS}
- Check the feasibility of your solution to ensure the above conditions.

OUTPUT FORMAT: After your solving, present your answer as:

{SOLUTION_FORMAT}

Where the PROBLEM_SPECIFIC_REQUIREMENTS are:

- TSP:
 - Must visit all the points exactly once, except the depot.
 - The start and end points must remain fixed.
 - The fixed path prevents any other visits in between; allow reversing of the fixed path where necessary.
- CVRP:
 - Must visit all the customer nodes exactly once.
 - Each route must start and end at the depot.
 - Vehicle capacity must not be exceeded.
 - The fixed path prevents any other visits in between; allow reversing of the fixed path where necessary.
- BPP:
 - Packed items' total weight in each bin must be less than or equal to the bin's capacity.
- MKP:
 - Selected items' total weight must be less than or equal to the knapsack's capacity.

And the SOLUTION_FORMAT should follow:

- TSP:

```
<sol>
  <route>0,1,2,...,0</route>
</sol>
```

- CVRP:

```
<sol>
  <route>0,1,2,...,0</route>
  <route>0,3,4,...,0</route>
  ...
</sol>
```

- BPP:

```

<sol>
  <bin_0>0,1,2,...</bin_0>
  <bin_1>3,4,...</bin_1>
  ...
</sol>

```

Where `bin_i` is the i -th bin.

- MKP:

```

<sol>
  <knapsack_0>0,1,2,...</knapsack_0>
  <knapsack_1>3,4,...</knapsack_1>
  ...
</sol>

```

Where `knapsack_i` is the i -th knapsack.

Reconstructor's User Prompt:

Reconstructor User Prompt

Given a set of `{ELEMENTS}`, your task is to find the `{OPTIMIZATION_OBJECT}` while respecting the following constraints.

`{CONSTRAINTS}`

Current solution:

`{SOLUTION}`

Where `ELEMENT` is set as:

- “nodes” for TSP and CVRP
- “items” for BPP and MKP

The `OPTIMIZATION_OBJECT` is set as:

- TSP: “Find the shortest possible tour that visits all nodes exactly once and returns to the starting depot.”
- CVRP: “Design a set of routes to deliver all customer demands using vehicles with limited capacity, minimizing the total distance while visiting each customer exactly once.”
- BPP: “Given a set of items with their weights, your task is to find the best packing solution that minimizes the number of bins used while respecting each bin’s capacity.”
- MKP: “Given a set of items with their values and weights, your task is to find the best packing solution that maximizes the total value while respecting each knapsack’s capacity.”

The `CONSTRAINTS` are:

- Routing problem (TSP and CVRP):
 - “Fixed visiting path as $(1,3), (5,9), \dots$ ” (i.e., some segments in the tour must be preserved).
- Packing problem (BPP and MKP):
 - Sum all items in the static segment s of each bin or knapsack, and treat them as a new bulky item, and set its weight

as the sum of item weights. For MKP, further set the bulky item’s weight and value as the respective sums.

`SOLUTION` in positive experience storage should include the current solution in the same XML format as required by the `SOLUTION_FORMAT` in the system prompt. If you have collected infeasible solutions by previous rounds, you can continue to append your user prompt:

Reconstructor User Prompt (append revision)

...

Analysis the following infeasible solution(s) and generate a new solution to meet the given constraints.

{INFEASIBLE_SOL1}

{INFEASIBLE_SOL2}

{INFEASIBLE_SOL3}

...

Where the template for negative experience `INFEASIBLE_SOLx` can be:

```

<sol>
  ...
</sol>
<reason>
  Missing visit node(s): 3, 7 ...
</reason>

```

B DETAILED EXPERIMENTAL RESULTS

B.1 TSPLIB Results

We then present full results on benchmarking instances from TSPLIB in Tables A3–A7 [add more commentary analysis](#)

OPRO fails to return valid solutions for all groups, as some hard instances in groups exceed the runtime limit, resulting in an infinite gap inf. SGE consistently produces infeasible solutions (infe), likely because it lacks explicit feasibility checks, since its original design is for small problems (under 30 nodes). LMEA handles slightly larger instances but exhibits high gaps and fails beyond 2k-node due to prompt length limits and generation timeouts.

B.2 CVRPLIB Results

Full results of CVRPLIB instances are listed in Tables A8–A9.

B.3 Ablation Studies

Ablation results analyzing decomposition and reconstruction strategies are provided in Table A10, and ablation results of LLM models are provided in Table A11.

B.4 Generalization Case Studies

BPP: Results are listed in Tables A12–A13. **MKP:** Performance are shown in Tables A14–A15.

Table A3: Result of DRAGON on the TSPLIB EUC_2D subset.

Size (k)	Name	Lower bound	Objective value	Gap (%)	#API calls	Input tokens (k)	Output tokens (k)	Running time (sec.)
<0.1	berlin52	7542	8773	16.322	18	352.398	27.373	1153.372
	eil51	426	440	3.286	25	355.136	33.297	1775.789
	eil76	538	598	11.152	27	584.812	45.871	1678.698
	pr76	108159	114421	5.790	16	293.463	20.841	929.784
	rat99	1211	1402	15.772	18	257.759	26.649	1827.705
0.1-0.2	st70	675	757	12.148	24	409.572	35.584	1757.166
	bier127	118282	135482	14.542	29	330.866	34.255	1957.364
	ch130	6110	6503	6.432	32	533.508	60.685	2831.500
	ch150	6528	7185	10.064	37	585.292	56.462	2719.040
	d198	15780	17621	11.667	46	871.951	67.258	3499.006
	eil101	629	694	10.334	40	705.357	70.520	2621.478
	kroA100	21282	23160	8.824	40	690.147	59.315	2354.898
	kroA150	26524	28278	6.613	36	502.292	47.662	1928.851
	kroB100	22141	23417	5.763	40	507.247	64.044	3507.437
	kroB150	26130	29267	12.005	9	223.708	17.918	613.975
	kroC100	20749	22964	10.675	20	370.270	32.169	1566.927
	kroD100	21294	22843	7.274	28	433.136	40.538	2048.876
	kroE100	22068	23402	6.045	23	415.897	37.632	1696.224
	lin105	14379	15979	11.127	17	198.105	22.608	1115.946
	pr107	44303	44925	1.404	22	200.629	27.529	1556.138
	pr124	59030	62151	5.287	22	386.629	35.707	1380.136
	pr136	96772	101634	5.024	18	301.971	24.507	1008.675
	pr144	58537	62220	6.292	18	347.802	25.506	932.202
	pr152	73682	77233	4.819	13	202.484	14.085	745.549
	rat195	2323	2588	11.408	26	438.158	47.778	2309.684
	rd100	7910	8865	12.073	27	555.131	48.948	1984.560
	u159	42080	47756	13.489	5	95.530	6.773	451.494
0.2-0.5	a280	2579	2901	12.485	19	358.893	27.183	988.452
	d493	35002	39490	12.822	38	685.977	67.881	3444.888
	f147	11861	12776	7.714	22	350.584	28.860	1451.702
	gil262	2378	2644	11.186	9	223.568	19.183	836.437
	kroA200	29368	31920	8.690	31	603.447	45.735	2069.374
	kroB200	29437	33157	12.637	40	803.297	74.733	3517.805
	lin318	42029	46716	11.152	31	660.784	46.946	2264.698
	pcb442	50778	58232	14.680	35	760.501	60.740	2542.813
	pr226	80369	81657	1.603	19	336.121	23.377	807.854
	pr264	49135	52991	7.848	29	574.093	49.003	1840.055
	pr299	48191	53787	11.612	18	333.709	30.133	997.101
	pr439	107217	121879	13.675	18	364.550	36.918	1166.819
	rd400	15281	17215	12.656	13	261.578	20.461	1039.604
	ts225	126643	144636	14.208	26	517.690	46.750	2419.392
	tsp225	3919	4324	10.334	9	152.992	15.664	789.163
0.5-1	d657	48912	54577	11.582	26	618.878	54.094	1999.693
	p654	34643	37476	8.178	19	518.997	32.475	1282.118
	rat575	6773	7590	12.063	49	1085.435	82.549	3511.544
	rat783	8806	9968	13.196	44	956.776	95.982	3505.717
	u574	36905	40922	10.885	28	779.953	40.176	1516.220
1-2	u724	41910	46740	11.525	16	342.380	18.580	982.001
	d1291	50801	60404	18.903	40	1640.458	61.223	2530.448
	d1655	62128	73834	18.842	14	456.675	32.196	1164.084
	f1400	20127	21521	6.926	33	920.564	98.208	3246.920
	f1577	22249	25526	14.729	5	69.703	10.569	243.459
	nrw1379	56638	63780	12.610	13	671.878	32.245	1241.157
	pcb1173	56892	65849	15.744	9	462.186	18.142	625.697
	pr1002	259045	293971	13.483	41	1609.575	62.281	2218.305
	rl1304	252948	302389	19.546	33	895.836	69.866	2343.211
	rl1323	270199	325813	20.583	22	846.612	42.888	1383.468
	rl1889	316536	376474	18.936	29	867.053	98.208	2627.414
	u1060	224094	248657	10.961	16	349.302	33.205	986.517
	u1432	152970	172925	13.045	22	1033.374	39.479	1447.544
	u1817	57201	68175	19.185	18	798.746	42.234	1986.882
2-5	vm1084	239297	267949	11.973	2	58.211	6.195	169.439
	vm1748	336556	380867	13.166	43	1271.237	88.938	3346.815
	d2103	80450	99775	24.021	23	888.182	74.305	2711.948
	f13795	28772	34268	19.102	26	1275.895	89.607	2589.477
	fnl4461	152566	207168	35.789	18	1289.366	34.595	1760.015
5-10	pcb3038	137694	158664	15.229	18	714.400	67.205	2618.376
	pr2392	378032	430293	13.824	38	1663.085	69.731	3113.234
	u2152	64253	77075	19.955	33	1061.294	108.541	3208.794
	u2319	234256	252285	7.696	21	632.640	78.352	2206.402
	rl5915	655530	688752	5.068	14	1385.583	67.902	1733.749
≥ 10	rl5934	556045	679642	22.228	18	3465.698	149.070	2340.457
	brd14051	469445	530915	13.094	24	2502.501	37.871	1950.459
	d15112	1573152	1780905	13.206	26	3877.022	49.884	2741.064
	d18512	645488	733860	13.691	2	525.051	2.558	1012.969
	rl11849	923368	1108759	20.078	12	1261.444	36.615	1398.704
	usa13509	19982889	22827898	14.237	22	3515.226	117.270	2748.211

Table A4: Result of LMEA on the TSPLIB EUC_2D subset.

Size (k)	Name	Lower bound	Objective value	Gap (%)	#API calls	Input tokens (k)	Output tokens (k)	Running time (sec.)
<0.1	berlin52	7542	22985	204.760	16	48.560	109.932	1633.713
	eil51	426	1194	180.282	24	71.568	174.415	1953.738
	eil76	538	1828	239.777	29	114.028	272.653	2818.638
	pr76	108159	396874	266.936	37	150.923	346.013	3486.687
	rat99	1211	6349	424.277	19	91.314	237.203	3511.408
0.1-0.2	st70	675	2710	301.481	33	122.232	289.233	3575.126
	bier127	118282	522377	341.637	23	140.829	306.311	3585.385
	ch130	6110	38924	537.054	22	131.648	226.152	3339.959
	ch150	6528	48726	646.415	10	67.440	67.322	992.652
	d198	15780	158386	903.714	18	160.992	232.834	2529.323
	eil101	629	2813	347.218	16	78.112	139.750	1630.725
	kroA100	21282	135707	537.661	26	129.116	272.577	3482.952
	kroA150	26524	218343	723.190	6	41.580	80.523	1077.787
	kroB100	22141	118419	434.840	35	174.020	412.730	3539.784
	kroB150	26130	202969	676.766	24	166.296	200.905	3093.957
	kroC100	20749	138488	567.444	16	79.440	174.127	2367.685
	kroD100	21294	129635	508.787	17	84.303	154.815	2220.916
	kroE100	22068	125387	468.185	35	174.020	413.782	3576.009
	lin105	14379	102517	612.963	9	46.071	97.868	1092.099
	pr107	44303	303855	585.856	22	117.128	285.457	3494.023
	pr124	59030	526278	791.543	19	114.076	213.121	3426.667
	pr136	96772	713073	636.859	14	90.776	163.846	1628.570
	pr144	58537	118820	102.983	23	156.492	350.591	3294.159
	pr152	73682	849178	1052.490	23	163.864	319.237	3442.378
	rat195	2323	19502	739.518	21	177.534	294.969	3588.559
	rd100	7910	44201	458.799	19	92.036	222.474	3590.330
	u159	42080	347796	726.511	21	155.484	294.184	3547.076
0.2-0.5	a280	2579	30832	1095.502	19	221.996	172.781	2004.626
	d493	35002	417749	1093.500	17	352.784	161.899	1966.156
	f417	11861	445256	3653.950	10	173.470	84.903	1325.056
	gil262	2378	24519	931.077	8	89.032	79.375	1085.446
	kroA200	29368	305520	940.316	16	142.192	168.055	2340.587
	kroB200	29437	289238	882.566	26	231.062	297.838	3578.618
	lin318	41345	544122	1194.635	8	108.504	89.533	837.863
	pcb442	50778	723164	1324.168	8	147.848	56.720	606.033
	pr226	80369	1442740	1695.145	21	212.100	198.219	1902.708
	pr264	49135	999930	1935.067	14	162.673	109.308	1553.069
	pr299	48191	677768	1306.420	23	299.092	272.404	3404.811
	pr439	107217	1781733	1561.801	8	148.960	96.041	1393.436
	rd400	15281	195457	1179.085	21	341.124	254.880	3520.224
	ts225	126643	1339414	957.630	33	331.980	428.714	3322.474
	tsp225	3919	30723	683.950	24	230.256	281.536	3326.143
0.5-1	d657	48912	816654	1569.639	8	218.376	78.842	810.460
	p654	34643	1892175	5361.926	8	217.760	82.629	1254.455
	rat575	6773	106143	1467.149	9	206.046	64.595	544.923
	rat783	8806	167368	1800.613	11	338.778	101.534	1243.282
	u574	36905	639997	1634.174	13	309.712	116.383	1127.479
1-2	u724	41910	814147	1842.608	13	387.374	125.961	1666.035
	d1291	50801	1659285	3166.245	9	515.853	129.673	1757.716
	d1655	62128	2123203	3317.466	10	782.590	106.926	976.751
	f11400	20127	1606464	7881.637	10	625.770	106.716	762.021
	f11577	22249	1310261	5789.078	8	584.680	125.307	1586.939
	nrw1379	56638	1370252	2319.316	10	626.630	92.113	1529.937
	pcb1173	56892	1362385	2294.686	8	402.384	114.889	1374.360
	pr1002	259045	6148455	2273.508	12	494.088	140.352	1893.208
	r11304	252948	8924001	3427.998	12	700.392	147.164	1848.956
	r11323	270199	7697390	2748.786	8	474.632	96.158	864.331
	r11889	316536	14023995	4330.458	16	1466.704	214.204	2081.738
	u1060	224094	6529359	2813.670	8	355.840	76.381	728.351
	u1432	152970	3772731	2366.321	15	985.260	184.622	2175.513
2-5	u1817	57201	2040136	3466.609	10	870.070	133.765	1910.557
	vm1084	239297	8130080	3297.485	13	594.997	168.779	1424.989
	vm1748	336556	14404027	4179.831	17	1421.727	220.912	2143.461
	d2103	80450	3136167	3798.281	8	828.416	95.846	974.011
5-10	f13795	28772	inf	inf	-	-	-	-
	fnl4461	152566	inf	inf	-	-	-	-
	pcb3038	137694	inf	inf	-	-	-	-
	pr2392	378032	14868838	3833.222	9	1083.636	62.958	893.720
	u2152	64253	2431659	3684.507	9	953.784	129.823	1924.544
	u2319	234256	5867710	2404.828	9	1046.187	79.161	1211.242
≥ 10	r15915	655530	inf	inf	-	-	-	-
	r15934	556045	inf	inf	-	-	-	-
	brd14051	469445	inf	inf	-	-	-	-
	d15112	1573152	inf	inf	-	-	-	-
	d18512	645488	inf	inf	-	-	-	-
	rl11849	923368	inf	inf	-	-	-	-
	usa13509	19982889	inf	inf	-	-	-	-

Table A5: Result of OPRO on the TSPLIB EUC_2D subset.

Size (k)	Name	Lower bound	Objective value	Gap (%)	#API calls	Input tokens (k)	Output tokens (k)	Running time (sec.)
<0.1	berlin52	7542	14774	95.899	9	12.420	2.428	61.642
	eil51	426	730	71.369	12	17.760	3.098	111.630
	eil76	538	1648	206.376	9	15.297	2.985	68.994
	pr76	108159	277854	156.895	15	32.916	4.802	157.505
	rat99	1211	3207	164.895	7	15.241	2.578	65.869
0.1-0.2	st70	675	inf	inf	-	-	-	-
	bier127	118282	inf	inf	-	-	-	-
	ch130	6110	inf	inf	-	-	-	-
	ch150	6528	inf	inf	-	-	-	-
	d198	15780	22512	42.664	9	41.007	4.905	65.386
	eil101	629	inf	inf	-	-	-	-
	kroA100	21282	inf	inf	-	-	-	-
	kroA150	26524	inf	inf	-	-	-	-
	kroB100	22141	157184	609.926	12	27.366	4.655	75.213
	kroB150	26130	273236	945.681	9	30.504	4.582	128.892
	kroC100	20749	inf	inf	-	-	-	-
	kroD100	21294	127458	498.564	27	72.300	9.721	267.155
	kroE100	22068	162325	635.569	9	21.474	3.301	96.389
	lin105	14379	inf	inf	-	-	-	-
	pr107	44303	74143	67.354	9	22.896	3.671	73.170
	pr124	59030	inf	inf	-	-	-	-
	pr136	96772	inf	inf	-	-	-	-
	pr144	58537	inf	inf	-	-	-	-
	pr152	73682	160979	118.479	9	31.986	4.099	119.534
	rat195	2323	inf	inf	-	-	-	-
	rd100	7910	inf	inf	-	-	-	-
	u159	42080	43375	3.079	9	33.348	4.138	77.461
0.2-0.5	a280	2579	2818	9.291	9	52.629	6.444	126.892
	d493	35002	inf	inf	-	-	-	-
	f4147	11861	inf	inf	-	-	-	-
	gil262	2378	inf	inf	-	-	-	-
	kroA200	29368	328171	1017.444	7	29.741	4.716	80.113
	kroB200	29437	327452	1012.384	9	40.176	5.487	164.678
	lin318	41345	119866	185.200	7	48.956	4.542	83.120
	pcb442	50778	542583	968.541	9	88.044	7.438	129.833
	pr226	80369	110416	37.386	9	46.860	6.380	103.985
	pr264	49135	77223	57.166	12	76.437	8.611	139.311
	pr299	48191	83507	73.285	18	121.149	13.592	289.296
	pr439	107217	inf	inf	-	-	-	-
	rd400	15281	215556	1310.617	9	74.589	6.980	173.999
	ts225	126643	1484736	1072.380	15	81.471	9.050	145.865
	tsp225	3919	inf	inf	-	-	-	-
0.5-1	d657	48912	inf	inf	-	-	-	-
	p654	34643	inf	inf	-	-	-	-
	rat575	6773	inf	inf	-	-	-	-
	rat783	8806	inf	inf	-	-	-	-
	u574	36905	inf	inf	-	-	-	-
	u724	41910	inf	inf	-	-	-	-
1-2	d1291	50801	inf	inf	-	-	-	-
	d1655	62128	inf	inf	-	-	-	-
	f1400	20127	inf	inf	-	-	-	-
	f1577	22249	inf	inf	-	-	-	-
	nrw1379	56638	inf	inf	-	-	-	-
	pcb1173	56892	inf	inf	-	-	-	-
	pr1002	259045	inf	inf	-	-	-	-
	rl1304	252948	inf	inf	-	-	-	-
	rl1323	270199	inf	inf	-	-	-	-
	rl1889	316536	inf	inf	-	-	-	-
	u1060	224094	inf	inf	-	-	-	-
	u1432	152970	inf	inf	-	-	-	-
	u1817	57201	inf	inf	-	-	-	-
	vm1084	239297	inf	inf	-	-	-	-
	vm1748	336556	inf	inf	-	-	-	-
2-5	d2103	80450	inf	inf	-	-	-	-
	f3795	28772	inf	inf	-	-	-	-
	fnl4461	152566	inf	inf	-	-	-	-
	pcb3038	137694	inf	inf	-	-	-	-
	pr2392	378032	inf	inf	-	-	-	-
	u2152	64253	inf	inf	-	-	-	-
5-10	u2319	234256	inf	inf	-	-	-	-
	rl5915	655530	inf	inf	-	-	-	-
	rl5934	556045	inf	inf	-	-	-	-
≥10	brd14051	469445	inf	inf	-	-	-	-
	d15112	1573152	inf	inf	-	-	-	-
	d18512	645488	inf	inf	-	-	-	-
	rl11849	923368	inf	inf	-	-	-	-
	usa13509	19982889	inf	inf	-	-	-	-

Table A6: Result of ReEvo(c) on the TSPLIB EUC_2D subset.

Size (k)	Name	Lower bound	Objective value	Gap (%)	Inference time (sec.)
<0.1	berlin52	7542	8608	14.140	0.034
	eil51	426	453	6.470	0.133
	eil76	538	579	7.620	0.190
	pr76	108159	120153	11.090	0.214
	rat99	1211	1361	12.410	0.199
0.1-0.2	st70	675	773	14.540	0.183
	bier127	118282	131049	10.790	0.521
	ch130	6110	6684	9.400	0.573
	ch150	6528	7234	10.820	0.705
	d198	15780	19247	21.980	1.614
	eil101	629	690	9.840	0.305
	kroA100	21282	22952	7.850	0.310
	kroA150	26524	29605	11.620	0.812
	kroB100	22141	24842	12.200	0.346
	kroB150	26130	29532	13.020	0.812
	kroC100	20749	24043	15.880	0.311
	kroD100	21294	23910	12.290	0.341
	kroE100	22068	23967	8.610	0.330
	lin105	14379	15215	5.820	0.337
	pr107	44303	47040	6.180	0.350
	pr124	59030	68244	15.610	0.568
	pr136	96772	108780	12.410	0.612
	pr144	58537	65538	11.960	0.704
	pr152	73682	83779	13.700	0.822
0.2-0.5	rat195	2323	2481	6.820	1.554
	rd100	7910	8665	9.550	0.208
	u159	42080	46487	10.470	0.946
	a280	2579	3067	18.930	4.387
	d493	35002	39701	13.430	22.934
	fl417	11861	14132	19.150	14.108
	gil262	2378	2685	12.940	3.699
	kroA200	29368	32620	11.080	1.635
	kroB200	29437	35024	18.980	1.687
	lin318	41345	49017	16.630	6.110
0.5-1	pcb442	50778	57607	13.450	16.612
	pr226	80369	94848	18.020	2.334
	pr264	49135	57378	16.780	3.528
	pr299	48191	58131	20.630	5.305
	pr439	107217	127860	19.250	16.301
	rd400	15281	17255	12.920	12.757
	ts225	126643	134946	6.560	2.236
	tsp225	3919	4350	11.020	2.319
	d657	48912	56758	16.040	54.088
	p654	34643	41121	18.700	53.232
0.5-1	rat575	6773	7638	12.780	36.041
	rat783	8806	10018	13.770	89.825
	u574	36905	44434	20.400	35.946
	u724	41910	48979	16.870	72.058
	d1291	50801	58731	15.610	402.530
1-2	d1655	62128	73008	17.510	850.869
	fl1400	20127	24096	19.720	494.310
	fl1577	22249	24944	12.110	734.272
	nrw1379	56638	64780	14.380	497.545
	pcb1173	56892	66840	17.490	308.277
	pr1002	259045	310008	19.670	189.077
	rl1304	252948	303725	20.070	421.773
	rl1323	270199	317559	17.530	439.428
	rl1889	316536	371919	17.500	1279.345
	u1060	224094	266469	18.910	223.714
	u1432	152970	172960	13.070	547.619
	u1817	57201	66718	16.640	1120.653
	vm1084	239297	280617	17.270	245.172
	vm1748	336556	396194	17.720	1024.559
2-5	d2103	80450	86631	7.680	1763.146
	f3795	28772	inf	inf	3600.101
	fnl4461	152566	inf	inf	3600.103
	pcb3038	137694	inf	inf	3600.029
	pr2392	378032	459589	21.570	2617.235
	u2152	64253	76497	19.060	1874.302
5-10	u2319	234256	248857	6.230	2318.946
	rl5915	655530	inf	inf	39401.084
	rl5934	556045	inf	inf	3600.103
	brd14051	469445	inf	inf	3600.107
≥10	d15112	1573152	inf	inf	3600.107
	d18512	645488	inf	inf	3600.109
	rl11849	923368	inf	inf	3600.096
	usa13509	19982889	inf	inf	3600.106

Table A7: Result of ReEvo(a) on the TSPLIB EUC_2D subset.

Size (k)	Name	Lower bound	Objective value	Gap (%)	Inference time (sec.)
<0.1	berlin52	7542	7549	0.100	1.873
	eil51	426	444	4.410	1.199
	eil76	538	561	4.310	1.276
	pr76	108159	116960	8.140	3.068
	rat99	1211	1287	6.350	3.670
0.1-0.2	st70	675	718	6.370	1.174
	bier127	118282	125723	6.290	2.270
	ch130	6110	6483	6.110	2.302
	ch150	6528	6767	3.670	6.842
	d198	15780	17404	10.290	3.839
	eil101	629	669	6.380	1.743
	kroA100	21282	22599	6.190	1.715
	kroA150	26524	29047	9.510	2.709
	kroB100	22141	23370	5.550	1.712
	kroB150	26130	29227	11.860	2.752
	kroC100	20749	21599	4.100	1.706
	kroD100	21294	22831	7.220	1.703
	kroE100	22068	23727	7.520	1.704
	lin105	14379	14954	4.000	1.818
	pr107	44303	47092	6.300	1.874
	pr124	59030	61293	3.830	2.217
	pr136	96772	108748	12.380	2.419
	pr144	58537	60957	4.140	6.187
	Pr152	73682	76744	4.160	5.508
0.2-0.5	rat195	2323	2481	6.810	3.734
	rd100	7910	8485	7.280	3.537
	u159	42080	44710	6.250	5.823
	a280	2579	2946	14.260	7.071
	d493	35002	38921	11.200	12.795
0.5-1	fl417	11861	13568	14.400	9.877
	gil262	2378	2618	10.100	10.935
	kroA200	29368	32150	9.470	8.430
	kroB200	29437	32924	11.850	8.610
	lin318	41345	47067	11.990	17.050
	lin318	42029	47067	11.990	17.050
	pcb442	50778	59216	16.620	25.854
	pr226	80369	89105	10.870	4.472
	pr264	49135	54196	10.300	5.357
	pr299	48191	53895	11.840	6.433
	pr439	107217	119854	11.790	22.855
	rd400	15281	17483	14.410	23.821
	ts225	126643	132257	4.430	4.455
	tsp225	3919	4306	9.880	9.928
0.5-1	d657	48912	56706	15.940	19.410
	p654	34643	41239	19.040	40.870
	rat575	6773	7789	15.000	15.848
	rat783	8806	10293	16.890	25.583
	u574	36905	43382	17.550	15.757
	u724	41910	48290	15.220	22.880
1-2	d1291	50801	58520	15.200	70.189
	d1655	62128	73286	17.960	161.547
	fl1400	20127	24131	19.900	50.081
	fl1577	22249	25637	15.230	134.016
	nrw1379	56638	67191	18.630	52.296
	pcb1173	56892	68553	20.500	91.328
	pr1002	259045	303407	17.130	80.787
	rl1304	252948	302084	19.430	94.308
	rl1323	270199	316894	17.280	48.574
	rl1889	316536	375685	18.690	86.597
	u1060	224094	269036	20.060	41.572
	u1432	152970	182777	19.490	107.057
	u1817	57201	65498	14.510	199.884
	vm1084	239297	283420	18.440	111.560
	vm1748	336556	406986	20.930	171.830
	d2103	80450	85620	6.430	103.428
	fl3795	28772	34390	19.530	212.787
	fnl4461	152566	221155	44.960	259.595
2-5	pcb3038	137694	166550	20.960	159.196
	pr2392	378032	458366	21.250	247.613
	u2152	64253	76332	18.800	100.445
	u2319	234256	272864	16.480	103.202
	rl5915	655530	686839	4.780	1019.255
5-10	rl5934	556045	674165	21.240	473.464
	brd14051	469445	577012	22.910	6294.430
	d15112	1573152	1943279	23.530	7639.086
	d18512	645488	794641	23.110	6152.544
	rl11849	923368	1130865	22.470	2086.743
≥ 10	usa13509	19982889	25269411	26.460	3008.846

Table A8: Result of DRAGON on the CVRPLIB (X/XML) subset.

Size (k)	Name	Lower bound	Objective value	Gap (%)	#API calls	Input tokens (k)	Output tokens (k)	Running time (sec.)
0.1-0.2	X-n110-k13	14971	19298	28.903	16	235.218	27.996	974.263
	X-n162-k11	14138	17280	22.224	15	330.999	31.953	792.177
0.2-0.5	X-n223-k34	40437	52877	30.764	13	249.044	23.135	710.500
	X-n284-k15	20226	26916	33.076	31	754.018	64.900	2080.547
	X-n420-k130	107798	133902	24.216	52	1238.116	110.004	3557.632
	X-n459-k26	24139	31597	30.896	32	1088.167	80.217	2263.910
0.5-1	X-n513-k21	24201	31918	31.887	39	1445.657	84.518	2477.514
	X-n670-k130	146332	211859	44.780	24	1181.644	75.815	2227.067
	X-n701-k44	81923	94156	14.932	6	251.993	15.387	454.379
	X-n783-k48	72386	94986	31.222	30	1117.956	88.571	2530.259
	X-n801-k40	73311	81258	10.840	26	971.698	53.939	1820.531
1-2	X-n1001-k43	72355	85873	18.683	48	1985.763	125.876	3510.914
	XML1000_1335_01	63968	73845	15.441	16	489.379	27.625	825.463
	XML1500_2114_01	99781	112163	12.409	24	1855.369	101.138	2936.169
2-5	XML2500_2145_01	112858	154727	37.099	23	1557.874	76.582	1948.524
	XML3500_3335_01	284329	300053	5.530	49	3397.328	161.908	3482.792
	XML4500_3233_01	602565	625500	3.806	32	3373.244	150.978	3480.450
≥ 5	XML5000_2224_01	315739	337855	7.005	28	5393.904	204.343	3549.789
	XML5000_1321_01	1466910	1566502	6.789	21	3137.194	91.763	2735.975
	XML5000_3135_01	396487	418520	5.557	26	2331.798	111.974	3028.920

Table A9: Result of ReEvo(a) on the CVRPLIB (X/XML) subset.

Size (k)	Name	Lower bound	Objective value	Gap (%)	Inference time (sec.)
0.1-0.2	X-n110-k13	14971	17758.55	18.620	3.293
	X-n162-k11	14138	17581.21	24.350	5.086
0.2-0.5	X-n223-k34	40437	47539.29	17.560	8.326
	X-n284-k15	20226	25702.50	27.080	11.032
	X-n420-k130	107798	122008.00	13.180	22.199
	X-n459-k26	24139	32910.35	36.340	21.046
0.5-1	X-n513-k21	24201	34441.10	42.310	24.540
	X-n670-k130	146332	179082.02	22.380	43.652
	X-n701-k44	81923	99286.02	21.190	40.841
	X-n783-k48	72386	101879.89	40.750	49.255
	X-n801-k40	73311	87669.11	19.590	49.812
1-2	X-n1001-k43	72335	94073.34	30.020	72.013
	XML1000_1335_01	63968	80300.27	25.530	69.735
	XML1500_2114_01	99781	120350.96	20.620	101.063
2-5	XML2500_2145_01	112858	164532.37	45.790	189.593
	XML3500_3335_01	284329	322280.75	13.350	289.669
	XML4500_3233_01	602565	643929.79	6.860	418.924
≥ 5	XML5000_2224_01	315739	359751.70	13.940	489.946
	XML5000_1321_01	1466910	1570524.76	7.063	567.689
	XML5000_3135_01	396487	446867.32	12.710	470.686

Table A10: Ablation for Decomposition and Reconstruction strategies

Decomposition	Reconstruction	Name	Gap (%)	Input tokens (k)	Output tokens (k)	Time (sec)
Heuristic	Heuristic	eil51	5.634	-	-	0.508
		pr299	12.83	-	-	1.043
		u1060	12.166	-	-	3.013
		brd14051	13.621	-	-	124.368
	Average		10.938	-	-	32.233
Random	Solver	eil51	5.634	-	-	1.118
		pr299	8.688	-	-	601.031
		u1060	12.374	-	-	602.940
		brd14051	13.386	-	-	724.978
	Average		10.021	-	-	482.517
LLM	LLM	eil51	7.981	66.143	10.258	101.244
		pr299	13.851	93.981	14.448	821.860
		u1060	11.173	89.304	11.820	656.243
		brd14051	13.196	276.588	25.373	1520.241
	Average		11.550	131.504	15.475	774.870
Heuristic	Heuristic	eil51	4.695	-	-	0.504
		pr299	15.688	-	-	1.056
		u1060	14.009	-	-	3.195
		brd14051	13.13	-	-	157.806
	Average		11.881	-	-	40.640
Heuristic	Solver	eil51	5.399	-	-	600.516
		pr299	10.207	-	-	701.056
		u1060	11.194	-	-	603.169
		brd14051	12.942	-	-	753.731
	Average		9.936	-	-	664.618
LLM	LLM	eil51	5.869	249.725	29.895	1653.207
		pr299	10.747	105.327	16.817	833.485
		u1060	13.170	75.322	15.279	1653.207
		brd14051	13.374	104.041	19.172	954.097
	Average		10.790	133.604	20.291	1273.499
Heuristic	Heuristic	eil51	5.634	196.966	9.220	407.764
		pr299	11.436	318.755	11.862	458.776
		u1060	10.961	420.500	17.615	462.020
		brd14051	13.094	1389.088	3.652	1081.917
	Average		10.281	581.327	10.587	602.619
LLM	Solver	eil51	5.634	188.621	10.222	535.234
		pr299	8.246	440.071	19.319	709.121
		u1060	10.961	352.112	28.451	642.717
		brd14051	13.079	10609.444	116.235	3260.043
	Average		9.480	2897.562	43.557	1286.779
LLM	LLM	eil51	3.286	355.136	33.297	1775.789
		pr299	11.612	333.709	30.133	997.101
		u1060	10.961	349.302	33.205	986.517
		brd14051	13.094	2502.501	37.871	1950.459
	Average		9.738	885.162	33.627	1427.466

Table A11: Impact of different LLM models

LLM model	Name	Gap (%)	#API calls	Input tokens (k)	Output tokens (k)	Running time (sec.)
gpt-4o	berlin52	16.322	18	352.398	27.373	1153.372
	kroB200	12.637	40	803.297	74.733	3517.805
	d2103	24.021	23	888.182	74.305	2711.948
	rl5934	22.228	18	3465.698	149.070	2340.457
	rl11849	20.078	12	1261.444	36.615	1398.704
	Average	19.057	22.20	1354.204	72.419	2224.457
deepseek-reasoner	berlin52	13.710	4	2.226	48.926	2431.104
	kroB200	14.190	4	5.031	45.960	2423.599
	d2103	23.052	2	22.289	25.028	2183.935
	rl5934	21.466	4	129.526	65.429	3036.950
	rl11849	inf	(Exceeds the model's max input limit)			
	Average	inf	-	-	-	-
o3	berlin52	3.248	20	10.425	182.739	3422.398
	kroB200	10.147	12	15.368	152.977	3343.023
	d2103	22.933	10	112.905	115.582	3220.190
	rl5934	21.672	14	456.244	105.146	2220.981
	rl11849	20.192	12	781.328	107.737	2150.865
	Average	15.638	13.60	275.254	132.836	2871.491
gpt-4.1	berlin52	6.457	12	7.011	13.566	289.156
	kroB200	8.900	13	18.041	17.039	284.020
	d2103	23.693	12	135.993	18.674	421.396
	rl5934	22.134	15	522.483	13.861	349.562
	rl11849	19.552	12	781.658	15.665	433.936
	Average	16.147	12.80	293.037	15.761	355.614

Table A12: Result of DRAGON for Bin Packing Problem.

Name	Objective value	L2 lower bound	Running time (sec.)	Gap (%)	# API calls	Input tokens (k)	Output tokens (k)
Weibull 5k/test_0	2020	2012	512.607	0.398	19	238.147	28.797
Weibull 5k/test_1	1984	1983	527.750	0.050	15	195.512	22.628
Weibull 5k/test_2	1990	1978	122.899	0.607	4	40.045	7.187
Weibull 5k/test_3	1992	1986	513.842	0.302	18	240.698	32.893
Weibull 5k/test_4	1986	1980	762.268	0.303	17	235.260	29.430

Table A13: Result of ReEvo(a) for Bin Packing Problem.

Name	Objective value	L2 lower bound	Running time (sec.)	Gap (%)
Weibull 5k/test_0	2079	2012	57.687	3.330
Weibull 5k/test_1	2052	1983	55.274	3.480
Weibull 5k/test_2	2050	1990	55.965	3.640
Weibull 5k/test_3	2053	1992	57.682	3.374
Weibull 5k/test_4	2049	1986	56.779	3.485

Table A14: Result of DRAGON for MKP.

Name	Objective value	Upper bound	Gap (%)	Running time (sec.)	# API calls	Input tokens (k)	Output tokens (k)
mkp_393_5_0	5427	5455	0.513	345.003	13	20.439	12.424
mkp_565_10_0	11415	11478	0.549	275.914	12	27.345	11.482
mkp_3594_20_0	37690	37706	0.042	159.304	12	143.961	6.545
mkp_3851_20_0	37018	37058	0.108	223.993	13	153.656	8.525
mkp_6870_50_0	83826	83880	0.064	213.504	12	275.633	12.221
mkp_6922_50_0	80305	80416	0.138	434.103	19	282.751	28.851
mkp_8864_50_0	85152	85266	0.134	320.866	16	350.271	17.373
mkp_10729_80_0	127696	127756	0.047	244.321	15	430.355	13.235
mkp_12397_50_0	105562	105592	0.028	123.530	7	240.881	5.239
mkp_30018_100_0	235436	235483	0.020	167.235	12	1152.107	3.960

Table A15: Result of OR-Tools (CP-SAT) for MKP.

Name	Objective value	Upper bound	Gap (%)	Running time (sec.)
mkp_393_5_0	5455	5455	0.000	2.52
mkp_565_10_0	11476	11478	0.017	3600.69
mkp_3594_20_0	37706	37706	0.000	80.11
mkp_3851_20_0	37058	37058	0.000	144.89
mkp_6870_50_0	83872	83880	0.010	3619.34
mkp_6922_50_0	80415	80416	0.001	3607.14
mkp_8864_50_0	85261	85266	0.006	3608.45
mkp_10729_80_0	127723	127756	0.026	3614.47
mkp_12397_50_0	105584	105592	0.008	3610.41
mkp_30018_100_0	227828	235483	3.251	3611.22